

<Original>

Natural Convection Flow and Heat Transfer in an Inclined Square Containing Internal Energy Sources

Jae Heon Lee* and Man Heung Park**

(Received December 24, 1983)

내부 발열을 갖는 경사진 정사각 공간에서의 자연대류유동 및 열전달

이 . 재 현 · 박 만 흥

초 록

균일하게 분포된 내부발열을 갖는 유체가 든 경사진(수평에서 45°까지) 정사각형 단면의 밀폐 공간 내에서의 2차원 자연대류 유동 및 열전달에 관한 수치적인 연구가 수행되었다. 4개 벽면온도가 동일한 경계조건에서 내부발열로 인한 자연대류 유동이 Rayleigh 수 1.5×10^6 까지는 층류유동 영역의 가정하에서 수치적으로 수렴 되었다. 경사진 밀폐 공간에서의 유동형태 및 온도분포는 수평인 경우에 비하여 윗쪽 벽면 근처에서 그 상이점이 많이 나타났다. 경사각도가 증가함에 따라 평균 열전달율이 아랫쪽 벽과 오른쪽 벽에서 증가하였고 왼쪽 벽에서 감소 하였으며 윗쪽 벽에서는 거의 일정 하였다.

Nomenclature

a	; Discretization constant	T	; Temperature
b	; Constant term in discretization coefficient	u, v	; Flow velocities in x and y direction
g	; Gravitational acceleration	x, y	; Cartesian coordinates
H	; Heat generation rate per unit volume	α	; Thermal diffusivity
k	; Thermal conductivity	β	; Isobaric coefficient of thermal expansion
L	; Width and height of enclosure	θ	; Inclined angle
Nu	; Local Nusselt number, eq.(12)	ρ	; Density
Nu^*	; Modified local Nusselt number, eq.(18)	ν	; Kinematic viscosity
\overline{Nu}	; Average Nusselt number, eq.(13)	ϕ	; General dependent variable
p	; Pressure	ψ	; Stream function
p'	; Modified pressure, eq.(1)	Subscripts	
Pr	; Prandtl number	L	; Left wall
q	; Local heat transfer rate per unit area	R	; Right wall
\bar{q}	; Average heat transfer rate per unit area	B	; Bottom wall
Ra	; Rayleigh number, $(g\beta/\alpha\nu)(L/2)^3(HL^2/8k)$	T	; Top wall
t	; Time	O	; Reference quantity
		+	; Conduction heat transfer mode

* Member, Dept. of Mechanical Engineering Hanyang University

** Member, Graduate School, Hanyang University

Superscripts

*	; Physical quantity
-	; Average value

1. Introduction

Thermal convection in an internally heated fluid layer has been considered as one of the major mechanism of nuclear reactor safety analysis^(1,2,3) as well as in geophysics⁽⁴⁾ and astrophysics^(5,6). Engineering processes where there is heat generation by a chemical reaction or a microwave heating within the fluid are common today such as manufacturing processes for resin-based materials. Kulacki and Goldstein⁽⁷⁾ have made the first experimental measurement of heat transfer from a layer containing heat generation with equal boundary temperatures. Recently transient phenomena have been reported by Keyhani and Kulacki⁽⁸⁾.

Natural convection in inclined enclosures also has been the subject of numerous investigations during the past decades. Earlier work on this problem has been presented systematically by Hart⁽⁹⁾. Recently Staehle and Hahne⁽¹⁰⁾ have extended their work to the transient natural convection.

So far, present author is not aware of any previous study dealing with natural convection in an inclined enclosure heated internally. The purpose of present work is to investigate the change of fluid motion, the temperature distribution and the heat transfer rate in according to inclined angle in a fluid with internal heat generation bounded by four isothermal walls.

For the present study, it is assumed that the fluid of steady-laminar flow satisfies the Boussinesq equation of state. In addition, the assumption of two-dimensional flow with the axis of the flow pattern has been made. This assumption has been experimentally verified by Ozoe et. al⁽¹¹⁾ for an externally heated square enclosure inclined at angle greater than 10 degree from horizontal.

Since results of present work need to experimental check-up, Prandtl number of 6.05 had been selected while this choice corresponds to diluted salt water which enables us to experiment. However, the effect of Prandtl number is not expected to be significant as shown by Jahn and Reinke⁽¹²⁾. Because the

section of enclosure is square and the boundary conditions of four walls are same, data are presented for the inclined angle from horizontal to 45 degree.

2. Mathematical Formulation

The inclined square enclosure is shown schematically in Fig.1. The isothermal walls of the enclosure maintain same uniform temperature during heat generation within it. The temperature and velocity

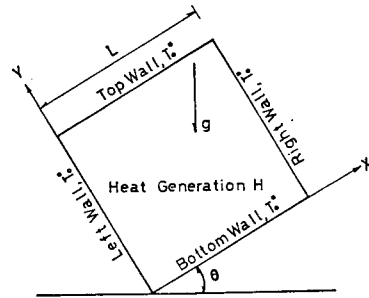


Fig. 1 Schematic representation of inclined square enclosure containing heat generation within it

fields within the fluid are governed by the continuity equation, the Navier-Stokes equations, and the energy equation. The steady-state solution could be obtained from long-time solution using following equation including time-dependent terms.

By defining a modified pressure p' as

$$P' = P^* + \{\rho_0^* g(1 + \beta T_0^*)\} (y^* \cos \theta + x^* \sin \theta) \quad (1)$$

and using Boussinesq approximation

$$\rho^* = \rho_0^* \{1 - \beta(T^* - T_0^*)\} \quad (2)$$

The equations can be expressed in non-dimensional form as

$$\frac{\partial u}{\partial x} + \frac{\partial v}{\partial y} = 0, \quad (3)$$

$$\frac{\partial u}{\partial t} + u \frac{\partial u}{\partial x} + v \frac{\partial u}{\partial y} = -\frac{\partial P}{\partial x} + \frac{\partial^2 u}{\partial x^2} + \frac{\partial^2 u}{\partial y^2} + \frac{Ra}{Pr} T \sin \theta, \quad (4)$$

$$\frac{\partial v}{\partial t} + u \frac{\partial v}{\partial x} + v \frac{\partial v}{\partial y} = -\frac{\partial P}{\partial y} + \frac{\partial^2 v}{\partial x^2} + \frac{\partial^2 v}{\partial y^2} + \frac{Ra}{Pr} T \cos \theta, \quad (5)$$

$$\frac{\partial T}{\partial t} + u \frac{\partial T}{\partial x} + v \frac{\partial T}{\partial y} = \frac{1}{Pr} \left(\frac{\partial^2 T}{\partial x^2} + \frac{\partial^2 T}{\partial y^2} \right) + \frac{2}{Pr}. \quad (6)$$

In equation (1) to (6), the following dimensionless variables have been used

$$x=2x^*/L, \quad y=2y^*/L, \tag{7a}$$

$$u=u^*/(2\nu/L), \quad v=v^*/(2\nu/L), \tag{7b}$$

$$p=p^*L^2/(4\rho^*\nu^2), \quad t=4t^*\nu/L^2, \tag{7c}$$

$$T=(T^*-T_0^*)/(HL^2/8k). \tag{7d}$$

$$Ra=\frac{g\beta}{\alpha\nu}(L/2)^3(HL^2/8k).$$

In equation (7d), $(HL^2/8k)$ indicates the maximum temperature difference which would occur in the layer with one-dimensional purely conductive heat transport between opposite walls. Boundary and initial conditions on velocities and temperature are next needed to complete the mathematical formulation of the problem posed by equations (3) to (6). As mentioned previously, the fluid is contained in a rectangular domain with four walls maintained same uniform temperature. Therefore, the thermal and hydrodynamic boundary conditions associated with equation (3) to (6) are,

$$x=0, 2; u=v=T=0 \tag{8a}$$

$$y=0, 2; u=v=T=0 \tag{8b}$$

The layer is assumed to be at a constant temperature and motionless at $t=0$. Thus, the initial conditions are,

$$u(x, y, 0)=v(x, y, 0)=T(x, y, 0)=0 \tag{9}$$

3. Solution Procedure

Equations (4) to (6) is discretized based on the control-volume formulation⁽¹³⁾. The final discretization equations have a generalized form on a grid point P

$$a_p \phi_p = \sum a_{nb} \phi_{nb} + b \tag{10}$$

where ϕ denotes the velocity or the temperature and the subscript nb denotes the neighbor grid points of p . The summation is to be taken over all the neighbors. In the present study, there are four neighbors.

The discretization equations are solved by a finite difference calculation procedure called SIMPLER (Semi Implicit Method for Pressure Linked Equations Revised)⁽¹⁴⁾. The main features of this method include a power-law formulation for the combined

convection-diffusion influence, an equation-solving scheme that consists of a block-correction method coupled with a line-by-line procedure, and a new algorithm for handling the interlinkage between the momentum and continuity equations.

A 32×32 grid was employed with a denser nodal point spacing near the walls. The results were determined to be grid independent by a comparison of the solutions obtained at successively finer grids.

In order to test the precision and accuracy of the numerical scheme of the present study, the balances between heat transfer rates through the every walls and heat generation rate within the fluid were checked. The agreements were considered very good. The largest difference in balances is less than 1.5%

4. Result and Discussion

Computer solutions were obtained in dimensionless form of velocities, temperature, pressure, stream function, local Nusselt number, and average Nusselt number. Results are presented in the forms of the stream line and isotherm contour plots, the distributions of local, average Nusselt number, and the value and location of the maximum temperature.

4.1. Streamline and Isotherm Patterns

The stream function is obtained from velocity field by evaluating the integral,

$$\phi = \int_0^y u dy \tag{11}$$

along constant- x lines and with $\phi=0$ along the walls. In Fig. 2 sixteen plots of streamlines are presented for Rayleigh number of 1.0×10^4 , 5.0×10^4 , 1.0×10^5 , and 1.5×10^5 at each inclined angle of 0 deg., 15 deg., 30 deg., and 45 deg.. It can be seen in inclined enclosure that the flow consists of two counter-rotating convective rolls and the fluid moves upward along the line paralleled with gravity which divides the whole cross-section area approximately half. This upward flow hits the top wall but the hitting point gradually shifts toward the upper top corner as the inclined angle increases. The streamlines at 0 deg. take on a different pattern. Owing

to secondary counter-rotating rolls in the upper portion, the main upward flow is blocked and divided by two. These two streams hit the top wall so that

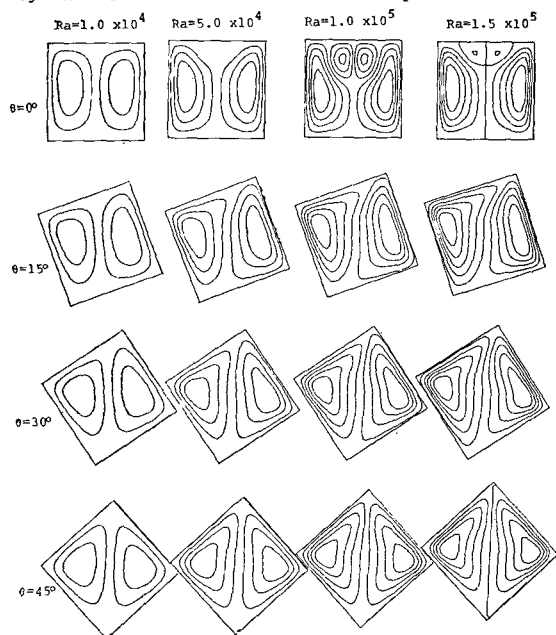


Fig. 2 Numerical streamlines. $Ra = 1.0 \times 10^4$, 5.0×10^4 , 1.0×10^5 , and 1.5×10^5 . $\theta = 0^\circ, 15^\circ, 30^\circ$, and 45°

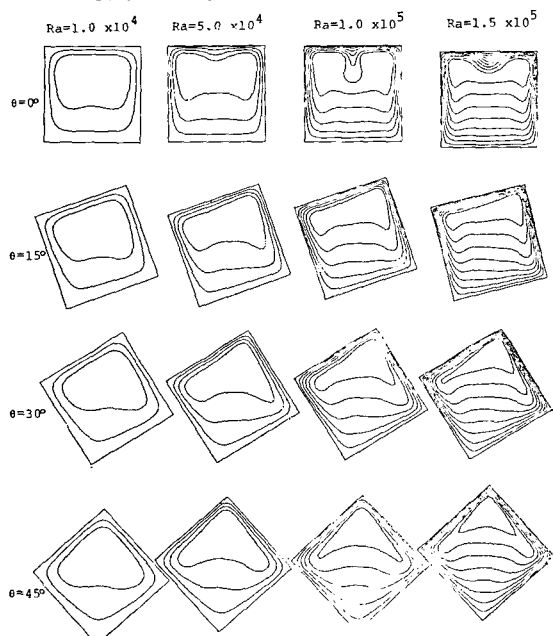


Fig. 3 Numerical isotherms. $Ra = 1.0 \times 10^4$, 5.0×10^4 , 1.0×10^5 , and 1.5×10^5 . $\theta = 0^\circ, 15^\circ, 30^\circ$, and 45° .

there exist two local maximum points of heat transfer rate.

For the same situations as streamlines, sixteen plots of isotherms are shown in Fig. 3. The temperature difference between each isotherms are 0.128, 0.073, 0.039, and 0.026 in dimensionless value and 0.009°C , 0.026°C , 0.027°C , and 0.026°C in dimensional value, for instance, using water properties for the Rayleigh number of 1.0×10^4 , 5.0×10^4 , 1.0×10^5 , and 1.5×10^5 respectively. When Rayleigh number is small as 1.0×10^4 , there are little influences due to natural convection so that the conduction mode in temperature profile prevails. Above 15° of inclined angle, as the angle increases, the temperature profile near the walls are almost fixed but the concavity of inner hotter profile becomes more large. This means that the natural convection has more influence upon the temperature distribution of inner space than that of outer space.

4.2. Heat Transfer

The local and average Nusselt number is defined using the half layer depth, $L/2$, as the characteristic length dimension and the aforementioned one-dimensional conductive maximum temperature, for example, in x -direction

$$Nu = \frac{\left| \frac{\partial T^*}{\partial x^*} \right|_{\text{wall}} \cdot \frac{L}{2}}{(HL^2/8k)} = \left| \frac{\partial T}{\partial x} \right|_{\text{wall}} \quad (12)$$

$$\overline{Nu} = \frac{1}{2} \int_0^2 Nu \, dx \quad (13)$$

In y -direction, ∂x or dx is replaced with ∂y or dy . There are four kinds of Nu called Nu_L , Nu_R , Nu_B , and Nu_T corresponding to the left, right, bottom, and top wall respectively. These subscripts are also used to differentiate from each \overline{Nu} . Actual heat transfer rate per unit area at each wall can be written as

$$q = HL \, Nu/4, \quad (14)$$

$$\bar{q} = HL \, \overline{Nu}/4. \quad (15)$$

Considering the heat balance, we can easily expect that the sum of \overline{Nu} on each wall must be 4. This fact was applied to check the accuracy of our results, as aforementioned.

Several plots of Nu distribution along each wall

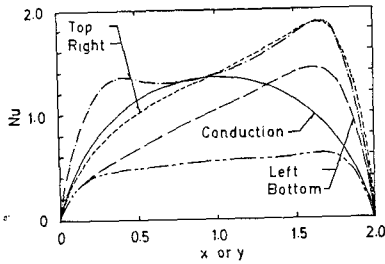


Fig. 4 Nu distributions of each wall. $Ra=1.0 \times 10^5$, $\theta=15^\circ$

are given in Fig. 4 at Rayleigh number of 1.0×10^5 and a inclined angle of 15° . The values are compared with the situation of conduction only mode in heat transfer. Along the top wall, Nu_r is higher than that of conduction. On the other hand, this state becomes reverse along the bottom wall. The values along the left and right wall are partially higher than those of conduction mode. These phenomena are caused by the fact that the hotter portion of fluid moves up due to buoyance.

The two local-maximum values on Nu_r can be seen in Fig. 4, which are caused by the flow pattern that would include the characteristics of the flow pattern within the horizontal enclosure. For inclined angle of 15° . at every Rayleigh number employed here, this two-local-maximum seems to remain.

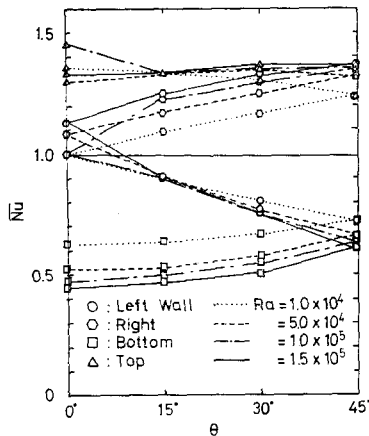


Fig. 5 Effect of inclined angle on \overline{Nu} of each wall for various Rayleigh numbers.

The variations of \overline{Nu} with inclined angle and Rayleigh number are shown in Fig. 5. The line of $\overline{Nu}=1$ which corresponds to that of conduction mode

only in heat transfer was drawn for comparison between convection and conduction. For the every Rayleigh number employed here, as the inclined angle increases from 15° , the magnitude of \overline{Nu} increases on the right and bottom walls but decreases on the left wall and keeps almost constant on the top wall. and as the Rayleigh number increases, on the top and right walls this value increases with $\overline{Nu} > 1$, on the contrary, on the bottom and left walls this value decreases with $\overline{Nu} < 1$. At 0° . of inclined angle the magnitude of \overline{Nu}_r shows somewhat different results. The value of \overline{Nu}_r at $Ra=1.0 \times 10^5$ is the highest one and the value of \overline{Nu}_r at $Ra=1.5 \times 10^5$ is lower than that at $Ra=1.0 \times 10^4$. This is presumably caused by complexity of flow pattern near the upper portion of symmetric line of the enclosure. However, the continuous investigation will be needed for this region further.

A comparison, in local heat transfer rate between that would occurs with convective flow and that would occurs with conduction only, is useful way to investigate the influences of natural convection. The conductive heat transfer rate per unit area at the top wall is determined as

$$q_+ = \frac{4HL}{\pi^2} \sum_{n=0}^{\infty} \frac{\sin[(2n+1)\pi x/2] \tanh[(2n+1)\pi/2]}{(2n+1)^2} \quad (16)$$

$$\bar{q}_+ = \frac{1}{2} \int_0^2 q_+ dx = HL/4. \quad (17)$$

Since heat transfer phenomena are symmetric with geometric center, equation(16) and (17) can be applied to the other walls with same manner.

The ratio (q/q_+) seems to be another useful quantity for engineering application. We define this ratio as modified local Nusselt number, Nu^+ ,

$$Nu^+ = q/q_+ = (Nu \cdot \pi^2) / \{16 \sum_{n=0}^{\infty} \frac{\sin[(2n+1)\pi x/2] + \tanh[(2n+1)\pi/2]}{(2n+1)^2}\} \quad (18)$$

The quantity corresponding to modified average Nusselt number is same as \overline{Nu} , since

$$\frac{1}{2} \int_0^2 Nu^+ dx = \overline{Nu}. \quad (19)$$

It is worth to mention here that the Nu is related to the absolute magnitude of heat transfer rate while the Nu^+ is related to the relative one to the conductive heat transfer rate. Among the computed results,

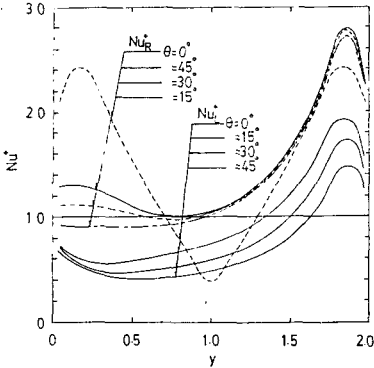


Fig. 6 Nu^+ distributions along the right and left walls. $Ra=1.5 \times 10^5$

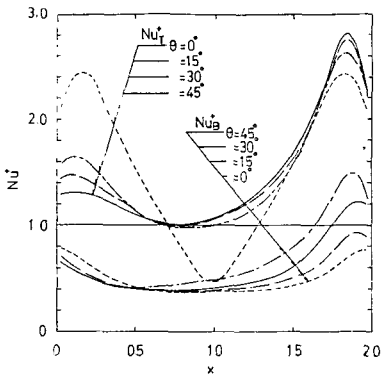


Fig. 7 Nu^+ distributions along the top and bottom walls. $Ra=1.5 \times 10^5$

the Nu^+ distributions along the each wall at $Ra=1.5 \times 10^5$ are shown in Fig. 6 and Fig. 7. The aforementioned behavior of the hotter portion within the inclined enclosure can be explained by the reason for Nu_{T^+} and Nu_{R^+} being greater than Nu_{B^+} and Nu_{L^+} . As the inclined angle increases, Nu_{B^+} becomes large near the right wall and Nu_{L^+} becomes small near the top wall but Nu_{R^+} and Nu_{T^+} keep almost same near the top wall and right wall respectively.

To investigate the Nu^+ variation with Rayleigh

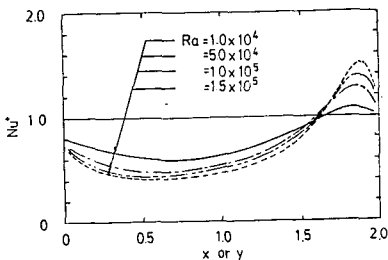


Fig. 8 Effect of Rayleigh number on Nu_{L^+} or Nu_{B^+}

number, inclined angle of 45 deg. is selected as typical example, see Fig. 8. As the Rayleigh number increases, the Nu_{L^+} ($=Nu_{B^+}$) decreases at the lower half portion of the enclosure but increases at the upper half portion of it. This means that the stronger convective flow within the inclined enclosure makes the steeper change in the heat transfer rate along the wall.

4.3. Maximum Temperature

The shift in position of maximum temperature and the value of it in the enclosure are additional interesting matter of present investigation. The relative value of this maximum temperature to that of which may occur in conduction only mode are given in Table 1. These relative values are always less than 1 and decrease as the Rayleigh number increases. Since the stronger convection gives the higher heat transfer rate through the walls, the temperature in the region of the hot fluid would decrease.

The positions of maximum temperature also can be seen in the contours of isotherms as shown in Fig. 2. Because of the symmetry, at horizontal enclosure, there are two locations which drift apart each other as the Rayleigh number increases. When the enclosure is inclined this position locates at $x^*/L=0.75$ and $y^*/L=0.75$ at $Ra=1.0 \times 10^4$ regardless, the angles. This position moves toward the upper top corner and reaches $x^*/L=0.85$ and $y^*/L=0.85$ at $Ra=1.5 \times 10^5$. By the through observation of isotherm patterns, this location seems to be a final location regardless of futher increase of Rayleigh number.

Table 1 The ratio of maximum temperature in convection to that in conduction mode only

Ra	$\theta=0^\circ$	$\theta=15^\circ$	$\theta=30^\circ$	$\theta=45^\circ$
1.0×10^4	0.646	0.654	0.661	0.660
5.0×10^4	0.496	0.499	0.497	0.497
1.0×10^5	0.393	0.439	0.436	0.436
1.5×10^5	0.401	0.404	0.399	0.397

5. Concluding Remarks

The problem of natural convection in an inclined square enclosure containing internal energy sources has been solved by a SIMPLER procedure.

The results indicate that the fluid moves upward along the line paralleled to gravity which divides the whole cross-section area half in case of $\theta=0$ deg. and 45 deg. but the direction of flow curve toward the top and bottom corner in case of $\theta=15$ deg. and 30 deg.. While the fluid moves downward along the side cold walls. In case of horizontal enclosure, the upward flow is blocked by the existance of secondary counter-rotating rolls before it hits the top wall.

The natural convection has more influence upon the temperature distribution of inner space than that of outer space. By the presence of natural convection within the inclined enclosure the average heat transfer rates on the top and right wall are higher than those of conduction only mode. On the contrary this situation becomes reverse on the bottom and left walls.

At the inclined angles of 0 deg. and 15 deg., there are two local maximums in the distribution of local heat transfer rate along the top wall. As the enclosure inclined from horizontal the flow-pattern has already changed before 15 deg. of inclined angle, but the trend in distribution of heat transfer rate still remains till this angle of inclination.

The maximum temperature occurs near the upper top corner within the inclined enclosure. Above 15 deg. of inclined angle, it is believed that the position of maximum temperature still locates at $x^*/L=0.85$ and $y^*/L=0.85$ even though in case of considerably high Rayleigh number.

References

(1) L. Baker, Jr., R.E. Faw, and F.A. Kulacki, "Postaccident Heat Removal-Part I: Heat Transfer Within an Internally Heated, Nonboiling Liquid Layer", Nucl. Sci. Engng., Vol. 66, pp. 223-230, 1976.
 (2) L. Baker, Jr., R.E. Faw, and F.A. Kulacki,

"Postaccident Heat Removal-Part II: Heat Transfer from an Internally Heated Liquid to a Melting Solid", Nucl. Sc. Engng., Vol. 66, pp. 231-238, 1976.
 (3) A.J. Suo-Anttila, and I. Catton, "The Effect of a Stabilizing Temperature Gradient on Heat Transfer from a Molten Fuel Layer with Volumetric Heating", ASME J. Heat Transfer, Vol. 97, pp. 544-548, 1975.
 (4) S.K. Runcorn, "Convection Current in the Earth's Mantle", Nature, Vol. 195, p.1248, 1962.
 (5) D.J. Tritton, "Internally Driven Heat Convection in the Atmosphere of Venus and in the Laboratory", Nature, Vol. 257, pp.110-112, 1975.
 (6) H.A. Bethe, "Energy Production in Stars", Science, Vol. 161, p. 541, 1968.
 (7) F.A. Kulacki, and R.J. Goldstein, "Thermal Convection in a Horizontal Fluid Layer with Uniform Volumetric Energy Sources", J. Fluid Mech., Vol. 55, pp. 271-287, 1972.
 (8) M. Keyhani, and F.A. Kulacki, "Experimentals on Transient Thermal Convection with Internal Heating-Large Time Results", ASME J. Heat Transfer, Vol. 105, pp. 261-266, 1983.
 (9) J.E. Hart, "Stability of the Flow in a Differentially Heated Inclined Box", J. Fluid Mech., Vol. 47, pp. 547-576, 1971.
 (10) B. Staehle, and E. Hahne, "Overshooting and Damped Oscillations of Transient Natural Convection Flows in Cavities", 7th Int. Heat Transfer Conference, Vol. 2, pp. 183-188, 1982.
 (11) H. Ozce, H. Sayama, and S.W. Churchill, "Natural Convection in an Inclined Square Channel", Int. J. Heat Mass Transfer, Vol. 17, pp. 401-406, 1974.
 (12) M. Jahn, and H.H. Reineke, "Free Convection Heat Transfer with Internal Heat Sources Calculations and Measurements", 5th Int. Heat Transfer Conference, NC 2.8, 1974.
 (13) S.V. Patankar, "Numerical Heat Transfer and Fluid Flow", Hemisphere Publishing, 1980.
 (14) S.V. Patankar, "A Calculation Procedure for Two-Dimensional Elliptic Situations", Numerical Heat Transfer, Vol. 4, pp. 400-425, 1981.